UDK 536.421.5:544.1:54-31:551.464
Original scientific article/Izvirni znanstveni članek

ISSN 1580-2949
MTAEC9, 55(5)629(2021)

SINTERING BEHAVIOUR OF MAGNESIUM OXIDE OBTAINED FROM SEAWATER DOPED WITH NANO-TiO_2

SINTRANJE MAGNEZIJEVEGA OKSIDA PRIDOBLJENEGA IZ MORSKE VODE DOPIRANEGA Z NANO TiO_2

Jelena Jakić*, Miroslav Labor, Vanja Martinac, Martina Perić

Faculty of Chemistry and Technology, Ruđera Boškovića 35, 21000 Split, Croatia

Prejem rokopisa – received: 2019-10-05; sprejem za objavo – accepted for publication: 2021-05-26

doi:10.17222/mit.2019.248

In order to improve the properties of sintered MgO (80 % precipitation) obtained from seawater, an investigation was carried out with (0, 1, 2) *w*/% of nano-TiO_2 and micro-TiO_2 additions during sintering at a temperature of 1500 °C (1 h and 2 h). The effects of the TiO_2 addition on its microstructural properties, density, porosity and chemical composition after sintering were observed. The SEM/EDS analysis confirmed the formation of a homogeneous microstructure composed mainly of periclase grains and well-distributed secondary phases. $CaTiO_3$ and $MgTiO_4$ are predominantly located at the inter- and intra-periclase grain boundary surfaces during cooling. The microstructure of the MgO samples with the addition of nano-TiO_2 become more compact, having a positive impact on the porosity and density of the samples. The addition of 1 *w*/% of nTiO_2 represents the optimal amount for the improvement of the properties of the MgO samples (80 % precipitation) obtained from seawater.

Keywords: seawater, nano-TiO_2, micro-TiO_2, porosity, density

Avtorji članka so poizkušali izboljšati lastnosti sintranega MgO pridobljenega iz morske vode (80 % izločanje). Postopek sintranja MgO so izvajali pri 1500 °C (1 in 2 uri) brez dodatka TiO_2, ter z dodatki 1 % in 2 % masnega deleža nano TiO_2 in mikro TiO_2. Po sintranju so opazovali kakšen je vpliv dodatka TiO_2 na mikrostrukturo, poroznost, gostoto in kemijsko sestavo. SEM/EDS analize so potrdile nastanek homogene mikrostrukture, sestavljene predvsem iz kristalnih zrn periklaza (kubična oblika MgO) in lepo porazdeljene sekundarne faze. Med ohlajanjem prevladujeta predvsem $CaTiO_3$ in $MgTiO_4$, locirana znotraj in na mejah kristalnih zrn periklaza. Mikrostruktura MgO vzorcev dopiranih z nano TiO_2 je bolj kompaktna, kar ima pozitiven vpliv na poroznost in gostoto vzorcev. Avtorji so ugotovili, da je 1 % masnega deleža TiO_2 optimalna količina dodatka za izboljšanje lastnosti sintranega MgO pridobljenega iz morske vode.

Ključne besede: morska voda, nano TiO_2, mikro TiO_2, poroznost, gostota

1 INTRODUCTION

Excellent physical and chemical properties enable a range of applications of MgO in the iron, steel, cement, glass and refractory industry. The properties of MgO refractories depend on the distribution and shape of grains, pores and purity of raw materials.[1] Additions of various additives have a significant effect on the improvement of properties. To increase the density of sintered MgO samples, additions of SiO_2, Al_2O_3, Fe_2O_3, Li_2O, TiO_2, ZrO_2 and halides such as LiF, LiCl are usually used.[2–6] An addition of LiF has a significant effect on the reduction of the sintering temperature and dielectric properties of MgO.[6] Also, recently the effects of V_2O_5, WO_3 and ZrO_2 additions as magnesium oxide sintering additives have been investigated.[7–9] An addition of activated carbon affects the magnesium oxide sintering process by reducing the activation energy of the sintering process and improving the sintering speed.[10] Small amounts of nano-additives such as Cr_2O_3, ZrO_2 and TiO_2 have also shown significant advances in improving the properties as well as the microstructure of magnesium oxide refractory materials.[11–13] The thermal-shock resistance and slag-corrosion resistance of MgO-CaO refractories were better improved with an addition of nano-ZrO_2.[11] Nano-TiO_2 affects the densification of sintered MgO-CaO samples and the grain growth of MgO and CaO, which further increases the hydration resistance and high cold crushing strength.[13]

The effect of a nanosized TiO_2 addition on the properties of MgO obtained from seawater had not been investigated before. Another investigation was made on the possibility of reducing the B_2O_3 quantity from sintered MgO samples, as much as possible, with a smaller nanosized TiO_2 addition. This study was carried out to improve the sintering process in order to obtain magnesium oxide with as low B_2O_3 and CaO content as possible and with good microstructure properties at the temperature of 1500 °C for durations of 1 h and 2 h and additions of 1 *w*/% and 2 *w*/% of nano- and micro-TiO_2.

2 EXPERIMENTAL PART

The materials used in this study were seawater (taken from the location of the Oceanographic Institute in Split, Croatia) and dolomite (taken from the location of Đipalo-Sinj, Croatia). The composition of seawater, de-

*Corresponding author's e-mail:
nina@ktf-split.hr (Jelena Jakić)

termined with the complexometric method,[14] was as follows:

2.1782 g/L MgO and 0.6116 g/L CaO, 0.0494 g/L CO_2, 4.37×10^{-3} g/L B

Dolomite lime was obtained with the calcination of dolomite at 950 °C for 5 h. The composition of the dolomite lime used as the precipitation agent was as follows:[15]

40.69 *w*/% MgO; 59.03 *w*/% CaO; 0.1083 *w*/% SiO_2; 0.0705 *w*/% Fe_2O_3; 0.0925 *w*/% Al_2O_3

Seawater was pre-treated with sulphuric acid in order to remove bicarbonate (HCO_3^-) and carbonate (CO_3^{2-}) ions, followed by the removal of liberated carbon dioxide (CO_2) with aeration in a desorption tower. The flow rate of the induced air was 120 L/h and the volumetric flow rate of seawater through the desorption tower was 6 L/h. After the pre-treatment of seawater, a calculated amount of dolomite lime was added to the magnesium hydroxide precipitate.

Processing seawater magnesium involves precipitation of magnesium hydroxide from the seawater, reacting with an alkaline base, such as calcined dolomite. The process involves the extraction of dissolved magnesium, which has a concentration of around 1.3 g/L in seawater, and the reaction of magnesium salts (chloride and sulfate) with dolomite lime to produce the magnesium hydroxide precipitate.

The experiments were carried out with substoichiometric precipitation, with an addition of 80 % of the stoichiometric quantity of dolomite lime.

The precipitation reaction with magnetic stirring took 30 min. Sedimentation was improved with the addition of the optimum amount (3.4 cm^3/L) of the anionic 818 A flocculent (polyacrylamide) produced by the Dutch firm Hercules. The optimum quantity of anionic 818 A flocculent was already described in a previous study.[16]

After the sedimentation of the magnesium hydroxide precipitate, the precipitate was decanted and rinsed. Distilled water (pH = 5.88) and alkalized distilled water (pH = 12.50) were used as the rinsing agent. Rinsing by decanting used a combined rinsing method (2 + 3), i.e., the magnesium hydroxide precipitate was rinsed 2 times with distilled water (pH = 5.88) and 3 times with alkalized distilled water (pH = 12.50). Rinsing by decanting was performed with about 1 L of the rinsing agent. The duration of the contact with the rinsing agent was about 30 min, i.e., until the precipitate settled again before the following decanting. After rinsing by decanting, the samples were rinsed in the process of filtering through multiple funnels using repeated rinsing (5 times) with distilled water (pH = 5.86). The rinsed precipitate was dried in an oven at 105 °C, and then calcined in a muffle furnace at 950 °C for 5 h to form caustic magnesia. **Table 1** shows the chemical composition of the magnesium oxide product (80 % precipitation).

Mixtures of magnesium oxide were then prepared with additions of of 1 *w*/% and 2 *w*/% of micro-TiO_2 and nano-TiO_2. The doping oxide used was analytical reagent grade titanium (TiO_2 p.a.) in the rutile form – produced by Carlo Erba Reagent (macro powder) and Aldrich Chemistry (nanopowder, < 100 nm particle size). Samples were homogenized by manual stirring in absolute ethanol for 30 min. The mixtures were dried at 80 °C until all alcohol evaporated. Mixtures were then cold pressed into compacts at a pressure of 625 MPa. Pressing was performed with a "Maschinenfabrik Herzog Osnabrück" hydraulic press, model TP 40. All compacts were sintered at the temperature of 1500 °C for durations of 1 h and 2 h. The time to reach this temperature in the gas furnace was about 2 h. After sintering, samples were left to cool down in the furnace (type 553, French company "Mecker").

Sintered MgO samples were characterized in terms of bulk density, apparent porosity, closed and total porosity. The bulk density and apparent porosity[17] were measured with the water-displacement method using the Archimedes' principle and calculated with Equations (1) and (2):

$$\text{Bulk density (g cm}^{-3}\text{):}\quad \rho = \frac{m_s}{V} \tag{1}$$

$$\text{Apparent porosity (\%):}\quad P_A = \frac{m_v - m_s}{\rho_{H_2O} \cdot V} \tag{2}$$

where m_s is the mass of the sample dried in air (g); V is the volume of the sample together with the bumps and cavities, i.e., the volume of the sample corresponding to the volume of water removed from the graduated cylinder (m^3); m_v is the mass of the sample soaked in water (g) and ρ_{H2O} is the density of water (g/cm^3). The results represent the average of a number of measurements (3 analyses in each case). The total and closed porosity[17] were calculated with Equations (3) and (4):

Table 1: Chemical composition of magnesium oxide obtained from seawater after calcination at 950 °C / 5 h

Sample	Rinsing agent	Number of rinses	CaO	MgO	B_2O_3
			w/%		
MgO (80 % precipit.)	Distilled water (pH = 5.88) + Alkalized distilled water (12.50)	By decanting (2 + 3)	1.43	96.53	0.072
	Distilled water (pH = 5.88)	On filter paper 5			
	Without rinsing the magnesium hydroxide precipitate	–	3.51	94.10	0.213

Total porosity (%): $P_t = \frac{\rho_t - \rho}{\rho} \cdot 100$ (3)

Closed porosity (%): $P_C = P_t - P_a$ (4)

Where ρ_t is the theoretical density (ρ_t = 3.576 g/cm^3). The boron content in the samples examined was determined using the potentiometric method. The variation coefficient for the method applied[18] is ± 1 %. The results represent the average of a number of measurements (5 analyses in each case). Magnesium oxide samples were also examined with scanning electron microscopy (JSM-6510 LV, JEOL) equipped with an attached energy dispersive X-ray spectrometer (Oxford INCA X-act.) for a semi-quantitative elemental analysis.

3 RESULTS AND DISCUSSION

In this study, micro- (mTiO$_2$) and nano-TiO$_2$ (nTiO$_2$) additions were used to determine new parameters of the sintering of MgO samples (80 % precipitation) as well as to improve their properties. The MgO samples (80 % precipitation) were sintered at the temperature of 1500 °C for durations of 1 h and 2 h. **Table 2** shows the effects of the TiO$_2$ addition on the bulk density of sintered samples. It was observed that the bulk density increases with an increase in the TiO$_2$ addition and sintering time. It is evident that the sintering time significantly affects the density of sintered MgO samples (80 % precipitation). Samples with nTiO$_2$ additions sintered for 1 h showed a slight increase in the density until after 2 h when the density increased significantly. Samples with an addition of 2 % mTiO$_2$ had a maximum bulk density of 3.448 g/cm^3, while those with a 2 % nTiO$_2$ addition had a maximum bulk density of 3.496 g/cm^3.

Table 2: Bulk density of sintered MgO samples (80 % precipitation) with 1 *w*/% and 2 *w*/% TiO$_2$, and with no sintering aid, τ = 1 h and 2 h, p = 625 MPa

Sample	τ / h	ρ /g cm^{-3}		
		ω (nTiO$_2$) = 0 *w*/%	ω (nTiO$_2$) = 1 *w*/%	ω (nTiO$_2$) = 2 *w*/%
MgO (80 % precipitation) 1500 °C	1	3.185	3.251	3.327
	2	3.414	3.448	3.496
	τ / h	ω (mTiO$_2$) = 0 *w*/%	ω (mTiO$_2$) = 1 *w*/%	ω (mTiO$_2$) = 2 *w*/%
	1	3.325	3.393	3.432
	2	3.377	3.433	3.448

The relative density of the sintered MgO samples (80 % precipitation) was determined as the ratio between theoretic (ρ_t = 3.576 g/cm^3) and measured density values, as shown in **Figure 1**. Maximum values of the relative density were obtained for the MgO samples (80 % precipitation) with 1 *w*/% and 2 *w*/% nTiO$_2$ additions sintered for 2 h at 1500 °C. These results show that the addition of TiO$_2$ promoted the densification of MgO samples (80 % precipitation), but the nTiO$_2$ addition had a better effect. The density increment in the MgO samples with nTiO$_2$ can be explained as the result of a better compaction between magnesia and calcia grains, better sintering of MgO samples due to the presence of fine reactive nanophases, and better mass transport due to the formation of new phases.[13]

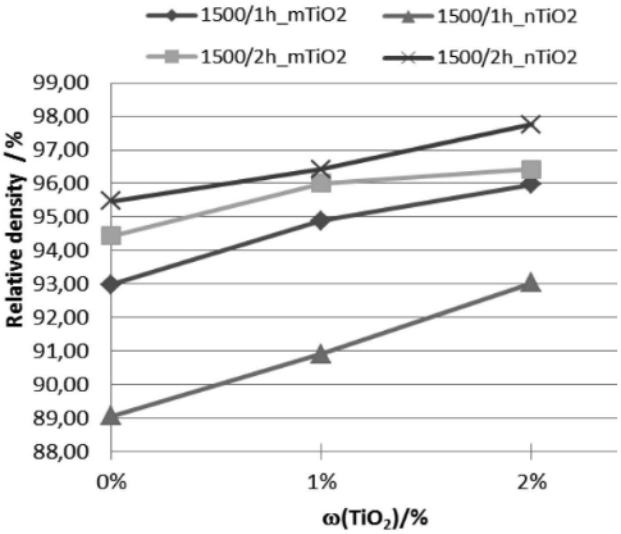

Figure 1: Relative density of sintered MgO samples (80 % precipitation) with 1 *w*/% and 2 *w*/% TiO$_2$, and with no sintering aid, τ = 1 h and 2 h, p = 625 MPa

When the density increases, the porosity of sintered MgO samples (80 % precipitation) decreases. **Figure 2** shows the experimental-porosity values. The examination results indicate a decrease in the open porosity with the increased sintering time, while the effect of the TiO$_2$ addition shows a deviation. At 1500 °C, with the addition of 1 *w*/% mTiO$_2$, the open porosity suddenly increases, while a further addition of the additive decreases the open porosity to 0.54 %. This can be explained by the effect of the B$_2$O$_3$ content in the sample of sintered

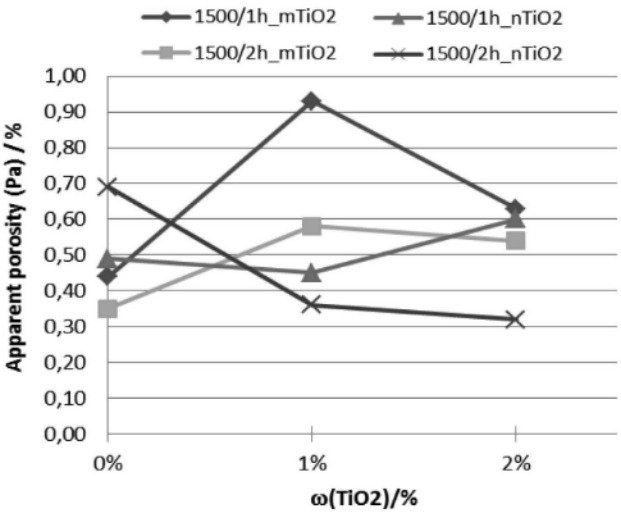

Figure 2: Apparent porosity of sintered MgO samples (80 % precipitation) with 1 *w*/% and 2 *w*/% TiO$_2$, and with no sintering aid, τ = 1 h and 2 h, p = 625 MPa

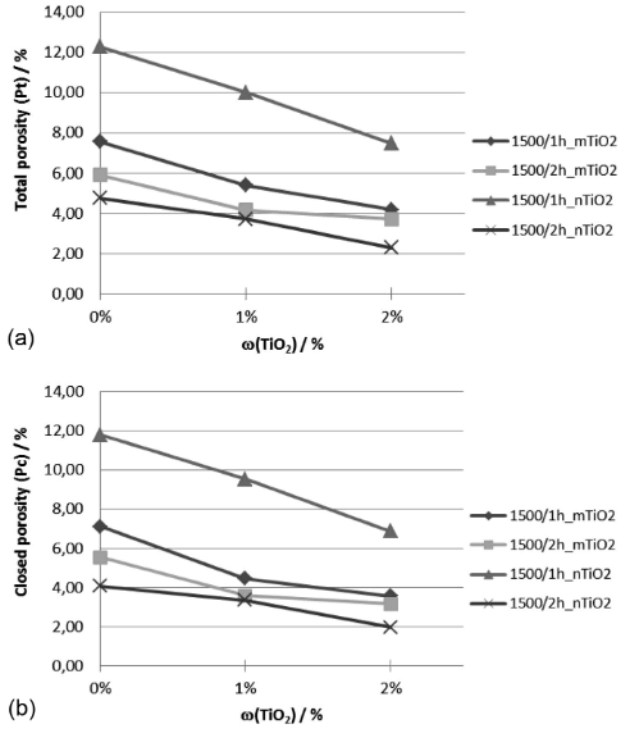

Figure 3: Total a) and closed b) porosity of sintered MgO samples (80 % precipitation) with 1 *w*/% and 2 *w*/% TiO_2, and with no sintering aid, τ = 1 h and 2 h, p = 625 MPa

MgO. Investigations so far[19] indicate that an increase in the time and $mTiO_2$ addition during sintering results in the evaporation of B_2O_3 from the sample into the atmosphere, thus reducing the open porosity. This increase in the open porosity with the addition of 1 *w*/% $mTiO_2$ is probably due to a slow evaporation of B_2O_3 at the temperature of 1500 °C. With the $nTiO_2$ addition, the apparent porosity is decreasing all the time with the increasing $nTiO_2$. The MgO sample (80 % precipitation) with 2 % of $mTiO_2$ has a minimum apparent porosity of 0.54 %; with $nTiO_2$, this value is 0.32 %. Minimum values for the apparent porosity were obtained for the MgO samples with 1 *w*/% and 2 *w*/% $nTiO_2$ additions sintered for 2 h at 1500 °C.

The total porosity and closed porosity (**Figure 3**) of sintered MgO samples do not show such deviations but an even decrease with the increase in the time and TiO_2 addition. The results for the total porosity with the $mTiO_2$ addition range from 7.54 % to 3. 70 %; with the $nTiO_2$ addition, they decrease down to 2.29 %, indicating a small number of open pores in the sample. The porosity values obtained indicate a better effect of the $nTiO_2$ addition during the isothermal sintering of MgO (80 % precipitation) from seawater.

Earlier studies[19,20] already showed that the $mTiO_2$ addition affects the B_2O_3 content in sintered samples of MgO obtained from seawater, but the effect of the addition of $nTiO_2$ has not yet been investigated. **Table 3** shows the results for the B_2O_3 content in sintered samples of MgO obtained with 80 % precipitation from seawater, with the addition of $nTiO_2$.

Table 3: B_2O_3 content in MgO samples derived from seawater (80 % precipitation), sintered at 1500 °C for 1 h and 2 h, with different additions of $nTiO_2$

	Sample	B_2O_3 (*w*/%)	
		τ = 1 h	τ = 2 h
1500 °C	MgO (80 %-precipitation)	0.069	0.067
	MgO (80 %-precipitation) + 1 *w*/% $nTiO_2$	0.0660	0.053
	MgO (80 %-precipitation) + 2 *w*/% $nTiO_2$	0.0136	0.013

The content of B_2O_3 in MgO samples is also affected by the method of rinsing the precipitate of magnesium hydroxide obtained with 80 % precipitation from seawater. Examinations were performed, using a combined method of rinsing the $Mg(OH)_2$ precipitate, i.e., a combined (2 + 3) method, rinsing twice with distilled water (pH = 5.88) and 3 times with alkalized distilled water (pH = 12.50) in the decantation process, and 5 times with fresh distilled water (pH = 5.88) on filter paper, relative to the CaO and B_2O_3 content and the amount of alkalized water spent. Already after the addition of 1 *w*/% $nTiO_2$ during 2 h of sintering at 1500 °C, the B_2O_3 content

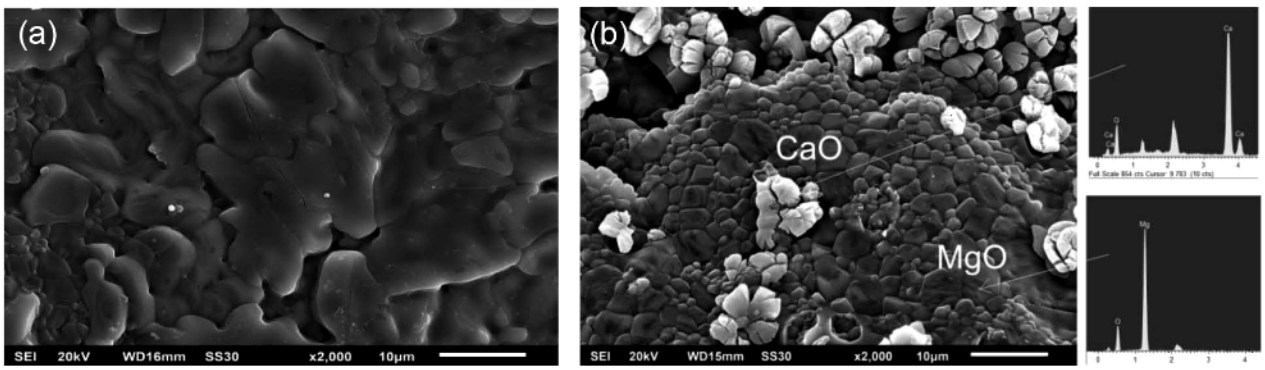

Figure 4: SEM images of samples of magnesium oxide (80 % precipitation) obtained from seawater without the addition of TiO_2, sintered at 1500 °C over two isothermal-sintering times: a) 1 h and b) 2 h

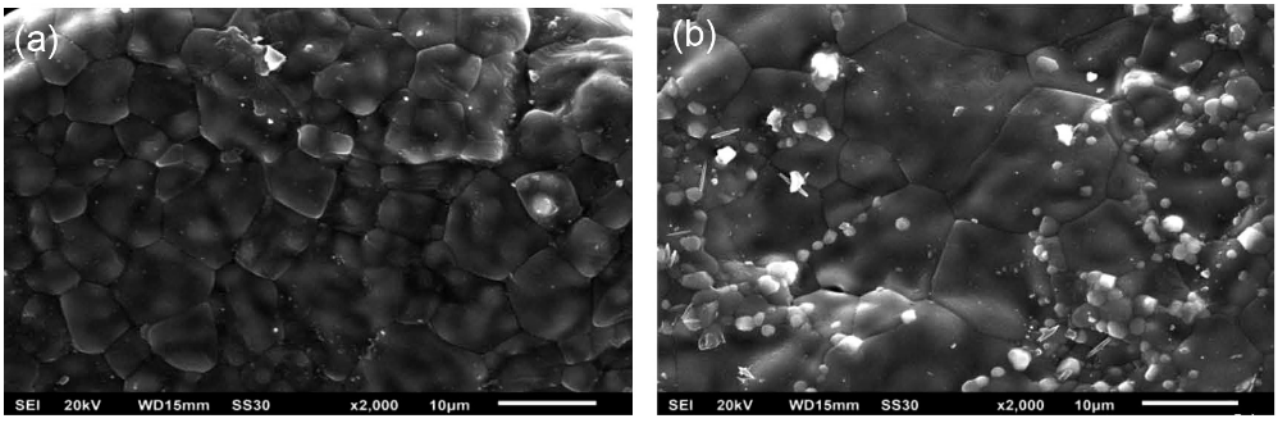

Figure 5: SEM images of MgO samples sintered at 1500 °C for 1 h: a) 1 *w*/% $nTiO_2$, b) 2 *w*/% $nTiO_2$

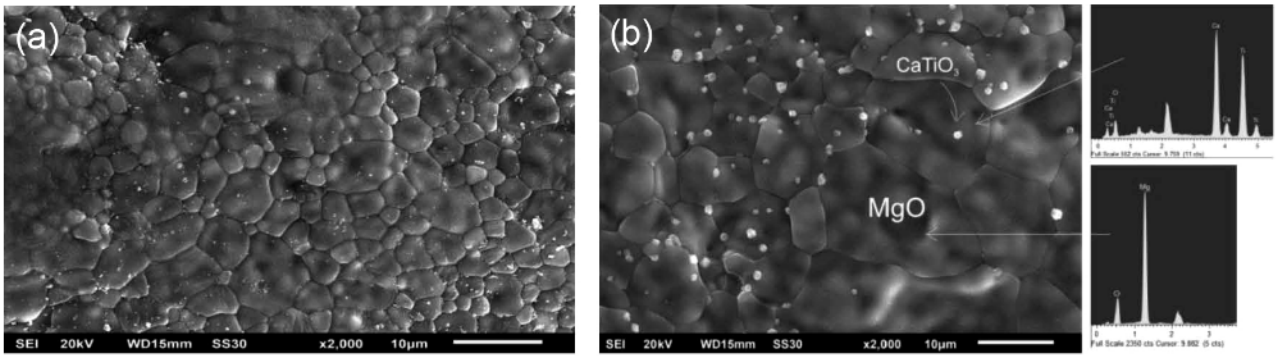

Figure 6: SEM images of MgO samples sintered at 1500 °C for 2 h: a) 1 *w*/% $nTiO_2$, b) 2 *w*/% $nTiO_2$

meets the requirements for high-refractory materials, which represents considerable savings in the technological process of producing sintered magnesium oxide.

According to N. Hesman, quality sintered magnesium oxide used in the refractory industry contains ≤ 0.05 % *w*/% B_2O_3.[21] Previous research[19] showed a noticeable decrease in the B_2O_3 content in sintered samples after the addition of 2 *w*/% $mTiO_2$ during 1 h and 2 h of sintering at 1500 °C, while the addition of 1 *w*/% had no significant impact. The addition of TiO_2 during sintering of MgO (80 %) changes the sample microstructure. Scanning electron microscopy (SEM) was used to determine the microstructure of the samples of MgO without the addition (**Figure 4**) and with the addition of $nTiO_2$ (**Figures 5** and **6**), sintered at 1500 °C, with the isothermal-sintering times of 1 h and 2 h. The EDS analysis confirmed the occurrence of new phases (**Figure 7**).

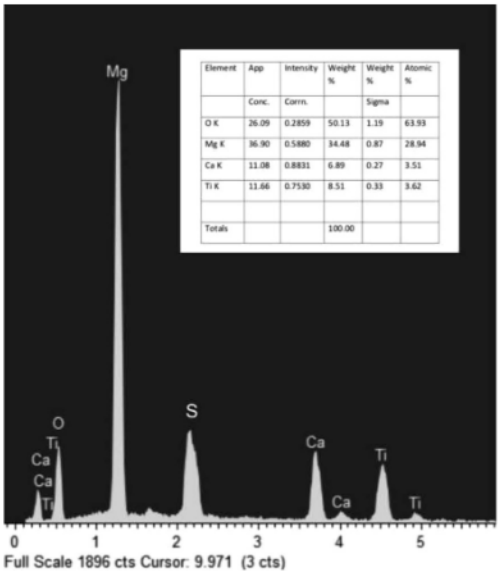

Element	App	Intensity	Weight %	Weight %	Atomic %
	Conc.	Corrn.		Sigma	
O K	26.09	0.2859	50.13	1.19	63.93
Mg K	36.90	0.5880	34.48	0.87	28.94
Ca K	11.08	0.8831	6.89	0.27	3.51
Ti K	11.66	0.7530	8.51	0.33	3.62
Totals			100.00		

Figure 7: EDS spectrum of MgO samples with the 2 *w*/% $nTiO_2$ addition, sintered at 1500 °C for 2 h

The SEM analysis shows a porous and non-homogeneous microstructure of the MgO samples without the addition of $nTiO_2$. The sintered sample without the addition has more pores and the periclase (dark grains) grains are smaller in size compared to the samples with $nTiO_2$. Periclase (dark phase) grains grew more rapidly than calcium (white phase) grains during the sintering process. It can be noted that pores were present at the boundaries between periclase and calcium grains or within the periclase grains (**Figure 4**). The addition of 1 *w*/% or 2 *w*/% $nTiO_2$ yields a more compact structure of the samples during sintering at 1500 °C for 1h (**Figure 5**). It is apparent that with the increase in the $nTiO_2$ addition and sintering time (**Figure 6**), the periclase grains increase and new secondary phases are formed, mostly at the grain boundaries.

The presence of Ca, O, Ti and Mg in the EDS spectrum (**Figure 7**) can indicate the formation of secondary phases. In the EDS spectrum, the peak at 2.2 eV belongs to sulphur. The presence of sulphur in the samples is due to the pre-treatment of seawater with sulphuric acid.

In previous studies, the XRD method detected only the formation of small amounts of $CaTiO_3$ and Mg_2TiO_4.[19] With the addition of $mTiO_2$, periclase grains increase, while formed $CaTiO_3$ and Mg_2TiO_4 separate in the form of thin layers on the periclase-grain boundary surfaces during cooling. A smaller amount of $CaTiO_3$ can also be observed within MgO grains.[19]

By applying small amounts of nanoparticles as additives, secondary phases are formed, mostly located at the matrix-grain boundaries and can create a pinning effect, i.e., blocking the grain growth during sintering. This effect favourably affects the mechanical properties of ceramic materials, especially the fracture strength and hardness.[22] **Figure 6b** shows the formation of secondary phases at the periclase-grain boundaries when $nTiO_2$ is added to sintered samples of MgO obtained from seawater. This pattern of secondary-phase formation results in blocking the growth of periclase grains and better binding of the periclase grains with secondary particles due to the increased temperature, sintering time and the addition of $nTiO_2$. The increase in the relative density, decrease in the porosity and better evaporation of B_2O_3 from the MgO samples with the addition of $nTiO_2$ can be attributed to the fine and homogeneous distribution of secondary phases and the pinning effect.

4 CONCLUSIONS

During sintering of MgO (80 % precipitation) from seawater, an addition of 2 *w*/% $mTiO_2$ gives a maximum relative density of 96.42 %, open porosity of 0.54 %, closed porosity of 3.7 % and total porosity of 3.16 %. If 2 *w*/% $nTiO_2$ is applied, the maximum value of relative density is greater, 97.76 %, while the porosity values are much lower: the open porosity is 0.32 %, closed porosity is 2.29 % and total porosity is 1.97 %, which is significantly lower than with the addition of $mTiO_2$.

The addition of TiO_2 is also important in view of the reduction of B_2O_3 in sintered samples due to the fact that during sintering, a part of CaO binds with calcium titanate ($CaTiO_3$), which leads to an increased B_2O_3 evaporation from the system during sintering. If 1 *w*/% $nTiO_2$ is used, after 2 h of sintering at 1500 °C, the requirements for the B_2O_3 content in a high-quality refractory material are met.

The changes in the microstructure are caused by a fine and homogeneous distribution of small amounts of secondary phases ($CaTiO_3$ and $MgTiO_4$) that have a favourable effect on the increased relative density, decreased porosity and better B_2O_3 evaporation from the MgO samples.

The addition of 1 *w*/% of $nTiO_2$ represents the optimal amount for the improvement of the properties of MgO samples (80 % precipitation) obtained from seawater.

5 REFERENCES

[1] R. H. R. Castro, K. Benthem, Sintering, Mechanisms of Convention Nanodensification and Field Assisted Processes, Springer, New York 2013

[2] T. Lucion, P. H. Duvigneaud, A. Laudet, J. F. Stenger, E. Gueguen, Effect of TiO_2 Additions on the Densification of MgO and MgO-CaO Mixtures, Key Engineering Materials, 268 (**2004**), 209–213, doi:10.4028/www.scientific.net/KEM.264-268.209

[3] Q. Z. Huang, G. M. Lu, Z. Sun, X. F. Song, J. G. Yu, Effect of TiO_2 on sintering and grain growth kinetics of MgO from $MgCl_2 \cdot 6H_2O$, Metallurgical and Materials Transactions B, 44 (**2013**), 344–353, doi:10.1007/s11663-012-9785-5

[4] V. Martinac, M. Labor, N. Petric, Effect of TiO_2, SiO_2 and Al_2O_3 on Properties of Sintered Magnesium Oxide from Sea Water, Materials Chemistry and Physics, 46 (**1996**), 23–30, doi:10.1016/0254-0584(96)80125-8

[5] V. Martinac, Effect of TiO_2 Addition on the Sintering Process of Magnesium Oxide from Seawater, In: A. Lakshmanan, ed., Sintering of Ceramics – New Emerging Techniques, InTech Europe, Rijeka 2012, 309–322, doi:10.5772/33748

[6] A. Kan, T. Moriyama, S. Takahashi, H. Ogawa, Low-Temperature Sintering and Microwave Dielectric Properties of MgO Ceramic with LiF Addition, Journal of Applied Physics, 50 (**2011**), 09NF02-1-5, doi:10.7567/JJAP.50.09NF02

[7] S. Kobel, D. Schneider, C. C. Schüler, L. J. Gauckler, Sintering of vanadium-doped magnesium oxide, Journal of the European Ceramic Society, 24 (**2004**), 2267–2274, doi:10.1016/j.jeurceramsoc.2003.07.009

[8] B. Han, Y. Li, C. Guo, N. Li, F. Chen, Sintering of MgO-based refractories with added WO_3, Ceramics International, 33 (**2007**), 1563–1567, doi:10.1016/j.ceramint.2006.07.014

[9] K. Das, S. Mukherjee, P. K. Maiti, P. G. Pal, Microstructural and densification study of natural Indian magnesite in presence of zirconia additive, Bulletin of Materials Science, 33 (**2010**), 439–444, doi:10.1007/s12034-010-0067-z

[10] Y. Xie, Z. Chen, Y. Wu, M. Yang, L. Weid, H. Hu, Activated sintering of activated carbon-doped magnesia, Ceramics International, 40 (**2014**), 16543–16547, doi:10.1016/j.ceramint.2014.08.008

[11] M. Chen, C. Lu, J. Yu, Improvement in performance of MgO-CaO refractories by addition of nano-sized ZrO_2, Journal of the European Ceramic Society, 27 (**2007**), 4633–4638, doi:10.1016/j.jeurceramsoc.2007.04.001

[12] H. R. Zargar, C. Oprea, G. Oprea, T. Troczynski, The effect of nano-Cr_2O_3 on solid-solution assisted sintering of MgO refractories, Ceramics International, 38 (**2012**), 6235–6241, doi:10.1016/j.ceramint.2012.04.077

[13] S. G. Kahrizsangi, A. Shahraki, M. Farooghi, Effect of Nano-TiO_2 Additions on the Densification and Properties of Magnesite-Dolomite Ceramic Composites, Iranian Journal of Science and Technology, Transactions A, (**2016**), doi:10.1007/s40995-016-0143-3

[14] K. Grasshoff, K. Kremling, M. Ehrhardt, Methods of seawater analysis, Wiley-VCH, Weinheim 1999

[15] J. Jakić, M. Labor, V. Martinac, Characterization of dolomitic lime as the base reagent for precipitation of $Mg(OH)_2$ from seawater, Chemical and Biochemical Engineering Quarterly, 30 (**2016**), 373–379, doi:10.15255/CABEQ.2015.2325

[16] N. Petric, V. Martinac, M. Labor, O. Jurin, Effect of 818A and 827N flocculants on seawater magnesia process, KZLTET, 33 (**1999**), 473–478

[17] HRN B. D8. 302, B. D8. 312, B. D8. 313: 1984

[18] F. Culkin, The major constituents of seawater, In: J. P. Riley, G. Skirrow, eds., Chemical Oceanography, 2nd ed., Academic Press, London 1975, 136–151

[19] J. Jakic, M. Labor, V. Martinac, The relationship between phase composition and conditions of sintering seawater derived magnesium oxide, Sadhana, 43 (**2018**), 119, doi:10.1007/s12046-018-0873-3

[20] M. Labor, V. Martinac, N. Petric, B_2O_3 content in the sintered magnesium oxide obtained from seawater, Indian Journal of Chemical Technology, 20 (**2013**), 276–281

[21] N. Heasman, New developments in seawater magnesia, Gas Wärme International, 28 (**1979**), 392–397

[22] P. Palmero, Structural Ceramic Nanocomposites: A Review of Properties and Powders' Synthesis Methods, Nanomaterials, 5 (**2015**), 656–696, doi:10.3390/nano5020656